



## SEISMIC PERFORMANCE INVESTIGATION OF BRACING AND SPD APPLICATION IN PHC PILE AS VIADUCT PIERS

A. S. Fajar<sup>(1)</sup>, M. F. Darmawan<sup>(2)</sup>, B. A. Yogatama<sup>(3)</sup>, I. Satyarno<sup>(4)</sup>, M. Guntara<sup>(5)</sup>

<sup>(1)</sup> Assistant Professor, Civil and Environmental Engineering Department, Gadjah Mada University, [angga.fajar.s@ugm.ac.id](mailto:angga.fajar.s@ugm.ac.id)

<sup>(2)</sup> Master Student, Civil and Environmental Engineering Department, Gadjah Mada University, [muhamad.fauzi.d@mail.ugm.ac.id](mailto:muhamad.fauzi.d@mail.ugm.ac.id)

<sup>(3)</sup> Geotechnical/Earthquake Engineer, Menard Asia, [bonifacius.adiguna@menard-asia.com](mailto:bonifacius.adiguna@menard-asia.com)

<sup>(4)</sup> Professor, Civil and Environmental Engineering Department, Gadjah Mada University, [iman.satyarno@ugm.ac.id](mailto:iman.satyarno@ugm.ac.id)

<sup>(5)</sup> Researcher and Engineer, PT Wijaya Karya Beton Tbk., [guntara@wika-beton.co.id](mailto:guntara@wika-beton.co.id)

### Abstract

In Indonesia, recently prestressed hollow concrete (PHC) piles are commonly used directly as the piers of elevated slab such as viaduct called pile-supported slab viaduct (PSSV). The application of PSSV is especially preferred in soft soil of rural area due its fast construction and economic cost. However, it is important to note that PHC piles have limited ductility so that they are not intended to response inelastically during major earthquakes. Based on the predecessor studies, PHC piles behave brittle manner in both axial force domination and flexural moment domination. This paper discusses an analytical study of additional steel bracing and also the one combined with shear panel damper (SPD) as the main seismic resistance and energy dissipation devices in some bays of PSSV structure. Those additional steel bracing and SPD is expected to avoid brittle failure mechanism in the PHC piles and to reduce structural drift under seismic excitation. In this study, two numerical model configurations of PSSV are developed by using displacement-based beam-column element with hinge in Opensees software, i.e. for the case of unbraced and braced with SPD. In the PHC pile element model, to consider the prestressed effect, initial stress is applied on the prestressing steel patch of the fiber section. Then, the SPD device to be idealized as link element with smoothed bi-linear material behavior following Manegotto-Pinto formulation. To quantify structural damping and energy dissipation of each structural configuration, five-step cyclic loading in a sequence interval of structural drift method was used. The equal damping ratio of the hysteresis loop is calculated based on the Jacobsen formulation. Furthermore, non-linear time history analysis was used to investigate the seismic performance of the PSSV structures with Newmark algorithm. The seismic excitation that used is a set of synthetic ground motions scaled to the maximum considered earthquake (MCE) for South Part of Java region. The synthetic ground motions consist of recorded and artificial acceleration time histories which were developed using point source stochastic method. The analytical results show that brittle failure in PHC piles occurred in unbraced PSSV structure. Meanwhile the application of additional steel bracing can increase the structural stiffness that reduces the structural drift and the application SPD will further reduce the structural drift as more energy dissipation can be achieved. Medium and slight inelastic responses were noted in the spun piles in PSSV with bracing only and PSSV with bracing and SPD respectively. This study successfully showed that the proposed PSSV structure braced with SPD addition had significantly higher seismic performance than the ordinary unbraced PSSV structure commonly used in elevated highway or railway infrastructure in Indonesia so that the proposed structure can be more feasible in serving the traffic load and have lower vulnerability to the earthquake.

*Keywords: spun pile, pile-supported slab viaduct, bracing, shear panel damper, seismic performance*



## 1. Introduction

Indonesia is one of the country with high earthquake risk. This is related to the position of Indonesia which is located in ring of fire containing about 13 segment of long belt subduction in South-West and North-East. Also, there are 251 active faults stand up in almost of Indonesia mainland [1]. Several significant earthquake in some Indonesia region has been well documented in last two years and caused huge losses and many casualties. More than 430 people have been confirmed dead after 6.9 magnitude earthquake hit Lombok Island in August 2018 [2]. Then, a powerful earthquake (6.1 magnitude of initial earthquake and 7.5 magnitude of main earthquake) which triggered a tsunami at Palu in September 2018 have killed more than 1200 people [3]. Furthermore, Halmahera Earthquake (7,2 Mw) had been recorded as the last significant earthquake occurred in July 2019, damaging hundreds of houses and killed 14 victims [4]. Therefore, the development of high seismic performance of building and infrastructure in Indonesia is a must to prevent the heavy damage caused by the collapse of the structures due to the earthquake. In otherwise, infrastructure of Indonesia are being developed rapidly to support the economic growth of Indonesia. One of them is toll road and railway track which commonly use pile-supported slab viaduct (PSSV) as illustrated in Fig 1 due its fast construction and economic cost. Pre-stressed hollow concrete (PHC) pile is generally utilized directly as the piers of PSSV structure. Based on predecessor studies, PHC piles have limited ductility and behave brittle manner in both axial force and moment flexural domination [5] [6]. But in other hand, PSSV structural design conducted by some experts or researchers in Indonesia used medium moment resisting concept [7] and no study about the external device addition to dissipate the energy of seismic motion, so that PSSV structure supported by PHC piles will have high risk in brittle collapse due to major earthquake. Budek et al recommended elastic design concept to be adopted for structural foundation using PHC pile in medium to high seismic risk zone to avoid brittle failure under seismic excitation [8].



Fig. 1 – Typical configuration of pile-supported slab viaduct and the application in Adi Soemarmo Airport Railway Track

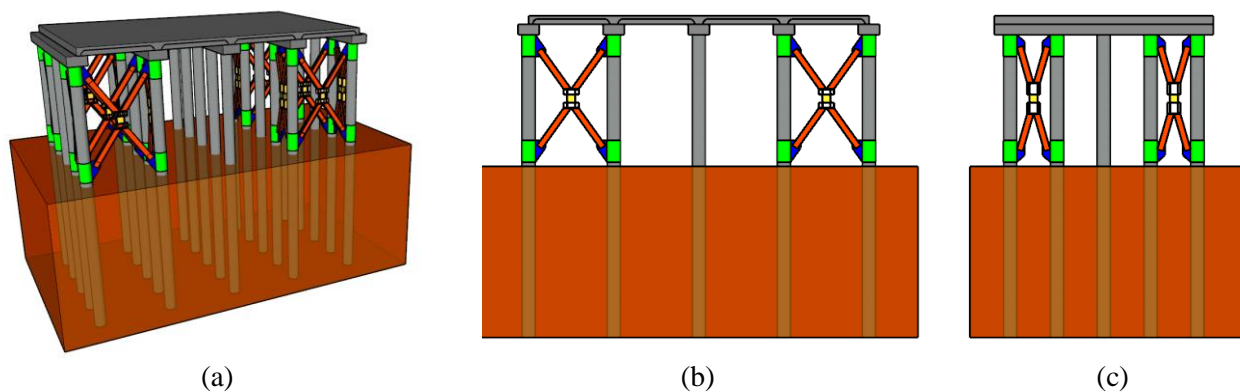


Fig. 2 – Proposed PSSV braced with steel bracing and SPD addition: (a) 3D view, (b) side view, (c) front view



In this study, PSSV structure braced structure utilized PHC piles as the piers with shear panel damper (SPD) addition in some bays was proposed. The proposed high seismic performance PSSV structure can be seen in Fig.2. An analytical study to investigate the seismic performance of the proposed structure was discussed. The SPD was expected to produce enough energy dissipation to damp the seismic excitation. The bracing connected the SPD to the structure. The combination of SPD and steel bracing was expected to increase the strength and the stiffness of the structure so that the structure can be more feasible in serving the traffic load and have lower vulnerability to the earthquake.

## 2. Numerical analysis method

### 2.1. Structural idealization

The PSSV structure was idealized as fiber section element in a three-dimensional model with six degrees of freedom, as illustrated in Fig.2. The numerical structure model has four bays in both x and z axes direction with 5000 and 2200 mm length of the span respectively. The red line showed in Fig. 2(a) means the bay braced with steel bracing and SPD addition. The eight meters length of PHC piles was modelled using displacement-based beam-column element. Fiber section was utilized to construct the section of the PHC piles. PHC piles fiber section consisted of a circular patch and circular PC bar layer. The circular concrete patch was divided to 72 and 20 fibers in the circumferential direction and the radial direction respectively. Beam elements connecting the top node of the PHC piles and steel bracing (double UNP profile) element were developed using elastic beam column element with section properties stated in Table 1.

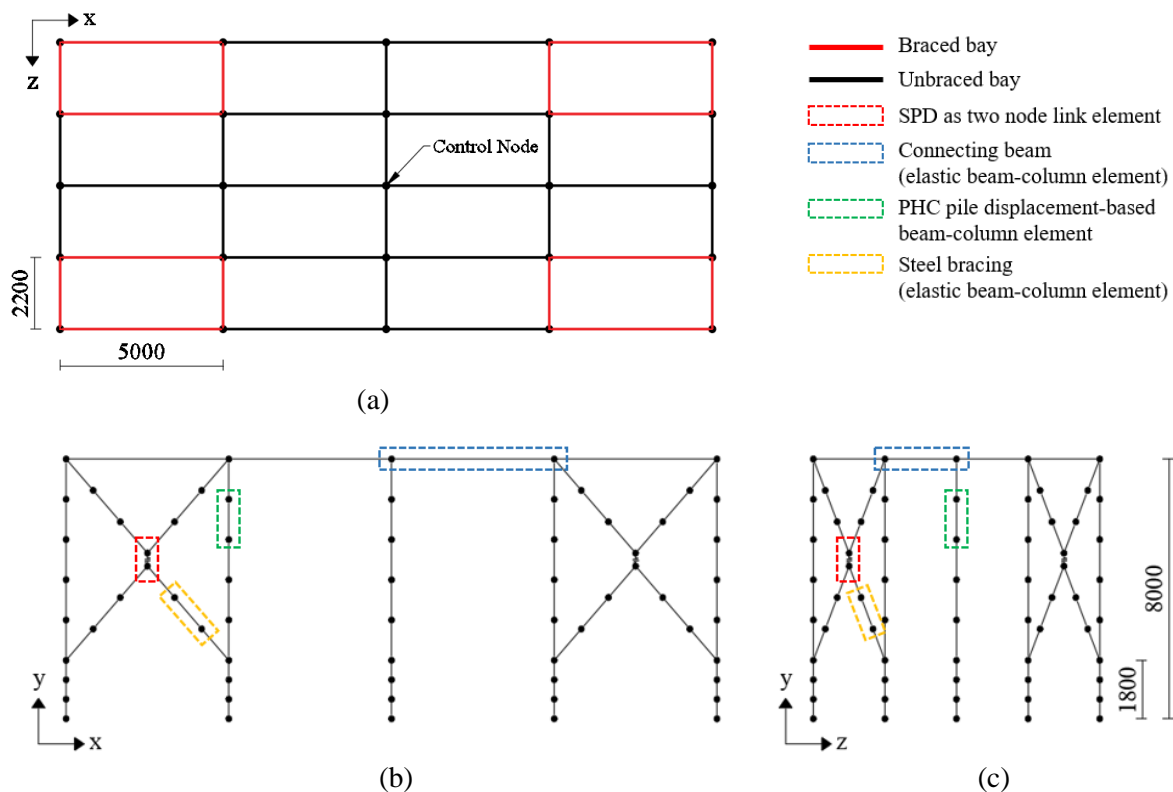


Fig. 3 – Structural idealization of PSSV: (a) top view, (b) side view, (c) front view

The PHC piles was assumed to be fixed in the lowest node. Nodal masses assigned at all top nodes of the PHC piles were 30.625 ton at middle node and 18.125 ton at edge node. RigidDiaphragm command was implemented to constraint certain degrees of freedom at the listed slave nodes (i.e. all node at the top PHC piles) to move as if in rigid x-z plane with the master node (i.e. Control Node). The control node was constrained in translation in y direction and rotation about x and z axes.

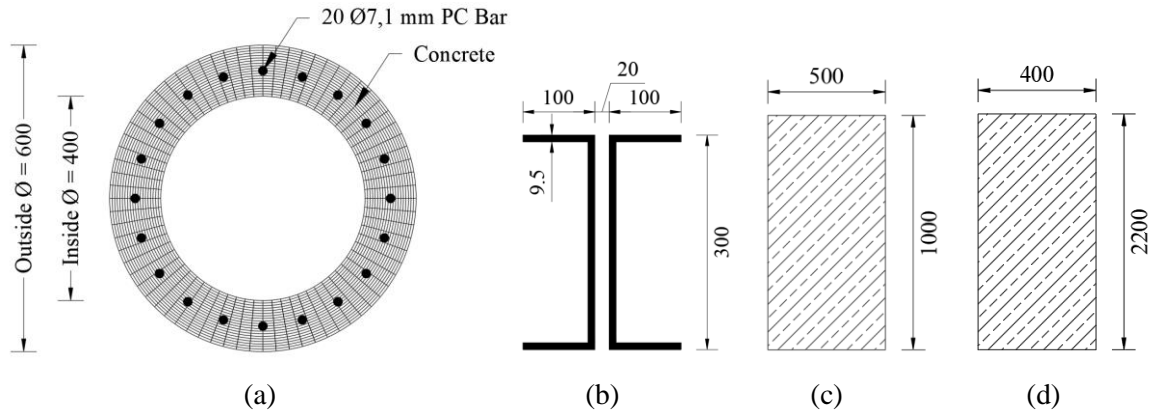


Fig. 4 – PHC piles fiber section (a), steel bracing section (b) and beam element section in z-axes direction (c) and x-axes direction (d)

Table 1 – Steel bracing and beam element section properties

Elastic beam column element parameter	Steel bracing element (double UNP profile)	Beam element z-axes direction	Beam element x-axes direction
Cross-sectional area of element, A (mm <sup>2</sup> )	9139	500000	880000
Young's modulus, E (MPa)	200000	36084.0359	36084.0359
Shear modulus, G (MPa)	76923.08	15035.016	15035.016
Torsional moment of inertia, J	264668.8	3.6667E+11	5.2083E+10
Moment inertia about the local z-axes, I <sub>z</sub> (mm <sup>4</sup> )	1.153E+08	3.5493E+11	4.1667E+10
Moment inertia about the local y-axes, I <sub>y</sub> (mm <sup>4</sup> )	18048387	1.1733E+10	1.0417E+10

Table 2 – Input parameter of (a) Concrete07 and (b) Steel02 for PHC pile material and two node element representing the SPD in x-axes direction (c)

(a) Concrete07		(b) Steel02		(c) SPD stiffness	
$f_c'$ (MPa)	54.40	$f_y$ (MPa)	1387.00	$k_x$ (N/mm)	6.943.E+06
$\epsilon_c$	0.002356	$E_0$ (MPa)	220200.00	$k_y$ (N/mm)	4.615.E+05
$E_c$ (MPa)	36699.78	$b$	0.05	$k_z$ (N/mm)	1.615.E+06
$\epsilon_t$	0.000248	$R_0$	10	$k_{\theta x}$ (Nmm/rad)	9.923.E+07
$x_p$	2	$cR_1$	0.925	$k_{\theta y}$ (Nmm/rad)	4.224.E+11
$x_n$	2.3	$cR_2$	0.15	$k_{\theta z}$ (Nmm/rad)	4.585.E+09
$R$	8.1				



## 2.2. Model of steel and concrete parameter of PHC pile fiber section

Chang and Mander's 1994 concrete model adopted in Concrete07 was implemented to model the PHC piles concrete material. The parameters of Concrete07 specified for the PHC pile were concrete compressive strength ( $f_c$ ), concrete strain at maximum compressive strength ( $\epsilon_c$ ), initial elastic modulus of the concrete ( $E_c$ ), tensile strength of concrete ( $f_t$ ), non-dimensional term that defines the strain at which the straight line descent begins tension and compression ( $x_p$  and  $x_n$ ) and parameter that controls the nonlinear descending branch ( $r$ ) [9]. Steel02 material based on Giuffre-Menegotto-Pinto model was adopted to model the behaviour of the PC bar. The input parameters were yield strength ( $f_y$ ), initial elastic tangent ( $E_0$ ), strain-hardening ratio ( $b$ ) and the parameters to control the transition from elastic to plastic branches ( $R_0$ ,  $cR_1$ ,  $cR_2$ ) [9]. The PC bar material parameters were selected referring to the experiment conducted by Irawan et al [10]. Table 2 list the input parameter of those concrete and steel material. To determine the PC bar pretensioning effect with magnitude 1101 MPa, Initial Strain material of OpenSees was adopted.

## 2.3. Shear panel damper model as link element

Shear panel damper (SPD) consist of welded steel plate, i.e. shear panel, flange frame and end plate [11]. SPD used in this paper was modelled by using two node link element command in OpenSees. The parameters defined were the stiffness corresponding each material directions: translations along local x,y,z axes and rotations about local x,y,z axes. Fig. 4 depicts SPD element added to the steel bracing in x-axes direction. Stiffness parameter of the x-axis SPD is listed in Table 2. While for SPD of z-axis direction steel bracings, the lateral stiffness and rotational stiffness about y-axis and z-axis was swapped.

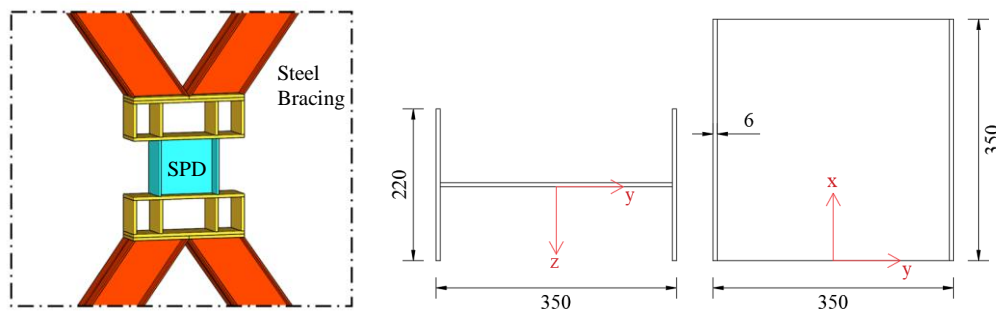


Fig. 5 – Shear panel damper (SPD) element added to the steel bracing in PSSV structure

## 2.4. Synthetic ground motion

Vast infrastructure development had emerged in Yogyakarta Province following the construction of the New Yogyakarta International Airport in Kulonprogo Regency. Yogyakarta and the surrounding area were devastated by the 2006 Mw 6.3 earthquake which was generated by the Opak Fault. The soil characteristic of Yogyakarta is mostly dominated by volcanic sand, ranging from loose to very dense with increasing depth. Loose sands near the ground surface contributed to many liquefaction observations during the 2006 event, as many buildings and roads were collapsed due to foundation failure from the liquefied sands. Based on these facts, Yogyakarta is one of the most seismically active area in Indonesia and thus selected for this study.

In order to perform the time history analysis, several ground motions with different characteristics were needed to investigate the performance of the studied structure under earthquake excitation. K-Net database was selected for the time history selection in this study. The time histories were selected based on the corresponding contributing earthquake for the area of interest, which was the result of a deaggregation analysis using PSHA (Probabilistic Seismic Hazard Assessment). For this study, the deaggregation analysis result from Sunardi [12] shown at Table 3 was used.

The contributing magnitude ( $M_w$ ) and hypocenter distance ( $R$ ) were used as the basis for selecting the time histories in the K-Net database. Monitoring station CHB011 (Hasunuma) was selected, since its soil condition is similar to the area of interest in this study (Fig. 6).



Table 3 – Deaggregation result for Yogyakarta with 2% probability of exceedance in 50 years ( $MCE_R$ ) [12]

	Shallow Crustal	Subduction
T = 0.2 sec	Mw 6.7, R = 15 km	Mw 7.1, R = 200 km
T = 1.0 sec	Mw 6.8, R = 17 km	Mw 7.4, R = 210 km

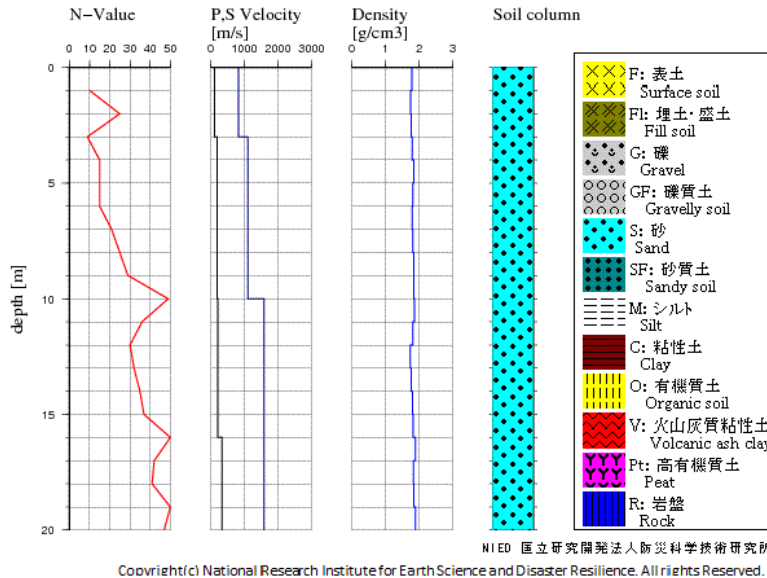


Fig. 6 – Geotechnical profile of station CHB011 (www.kyoshin.bosai.go.jp)

From the database, only two earthquake events satisfied to the deaggregation criteria as shown in Table 4 above, which can be summarized below.

Table 4 – List of selected earthquake event

	Earthquake 1	Earthquake 2
Magnitude	Mw 7.4	Mw 6.1
Easting	141.60E	140.93E
Northing	37.35N	35.75N
Depth	25 km	15 km
Epicentral Distance	219 km	42 km
Date	22/11/2016	14/3/2012
Time	05:59	21:05

The above earthquake already has two different characteristics for the recording site: Earthquake 1 came from subduction source with has long propagation distance and high magnitude, which resulted in high energy over the low frequency range, while Earthquake 2 came from a shorter source distance (active shallow crustal fault) which lead to high energy over the high frequency range. These two different slip mechanism and propagation characteristics are similar to the deaggregation result for Yogyakarta. The shallow crustal source will be very likely come from the Opak Fault, while the subduction source is coming from the Megathrust subduction zone south of Java.

Having only two acceleration records was not enough to study the structural dynamic behavior. To complement the two records, a synthetic ground motion modeling using point source stochastic approach [13] was performed. Two acceleration time histories representing the shallow crustal source and one for the subduction source were modelled. The generated ground motions from the stochastic approach were



referenced to outcropping bedrock ( $V_s = 750$  m/s). In order to get the acceleration at ground surface, nonlinear site response analyses were performed for the soil profile as shown in Fig.6. The shear modulus reduction and damping curve from Seed and Idriss [14] were used considering the mean curves.

All acceleration time histories (recorded and synthetic) were then baseline corrected and filtered before getting scaled to match the design response spectrum as suggested by SNI 1726-2012. The waveform and response spectrum of the processed ground motions are presented in Fig. 7 and Fig. 8, respectively. The recorded motions are denoted as “Earthquake 1” and Earthquake 2”, while the artificial motions are denoted as “Shallow 1”, “Shallow 2”, and “Subduction”.

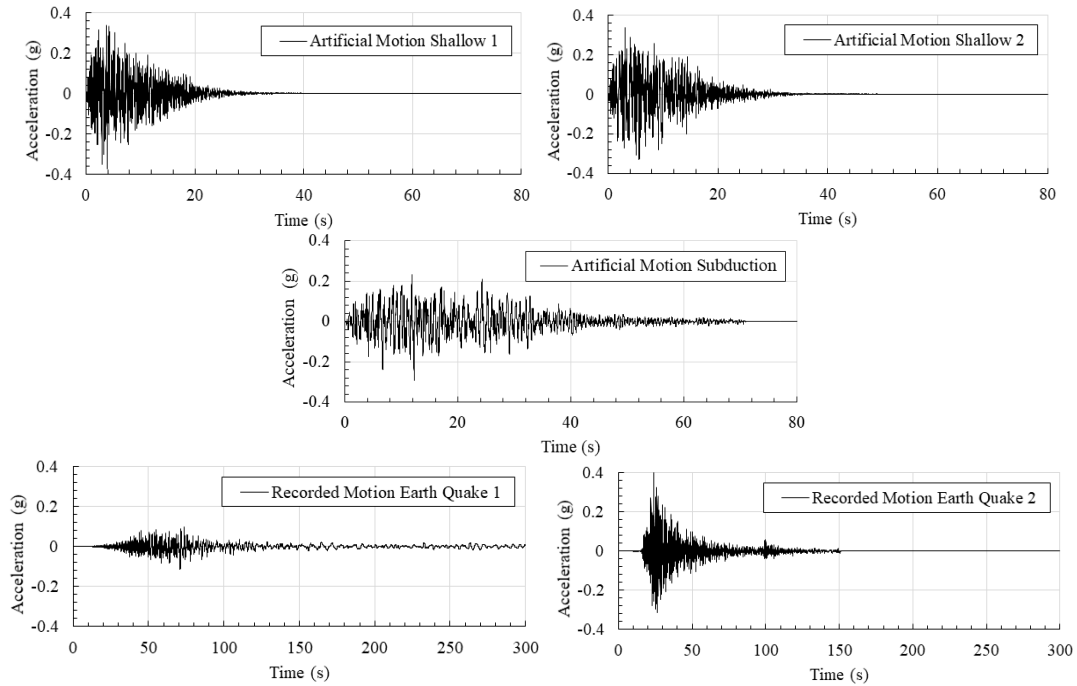


Fig. 7 – Artificial and recorded earthquake ground motion

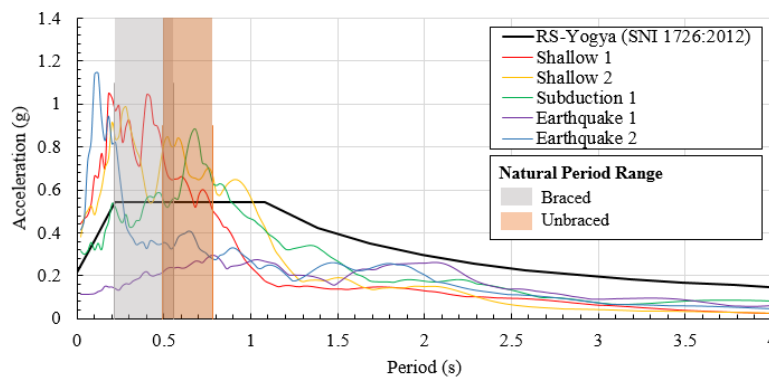


Fig. 8 – Response spectrum of seismic excitation

2.5. The structural performance investigation method

Non-linear analysis include static pushover, cyclic loading analysis and dynamic time history analysis was performed to observe the structural behavior and performance, respectively. This study only consider the PSSV structure in longitudinal direction. Each of those analysis were preceded with eigenvalue analysis to obtain the natural periods of the structure and gravity analysis stage in the form of constant nodal load pattern in the gravity direction. Cyclic loading analysis was conducted by applying continuously increasing sinusoidal waves shown at Fig.9. There are ten steps of displacement loading protocol to the control node.



During cyclic loading, equal damping ratio of PSSV structure was calculated with Jacobsen's approach expressed by Equation 1 [15].  $A_{hyst}$  is the energy dissipation area of the hysteresis loop in a cycle loading then  $A_0$  is the twice area of elastic strain energy.

$$\zeta = \frac{1}{2\pi} \frac{A_{hyst}}{A_0} \quad (1)$$

Also, static pushover analysis was run to examine the skeleton curve characteristic and the limit state of the structure i.e.: concrete crushing limit, PC bar yielding and ultimate limit and SPD yielding limit. Furthermore, time history analysis from several dynamic uniform earthquake synthetic ground motions was performed to find out the structure response under those seismic excitation. Newton algorithm of load integrator was utilized under both of the gravity, cyclic loading and static pushover analysis. No time increment applied in the gravity loading analysis, while time increment 0.01 s and 0.001 s was defined in the cyclic loading and static pushover analysis, respectively. Otherwise, Newmark integration method was implemented in the dynamic analysis with time increment 0.005 s and 0.01 s.

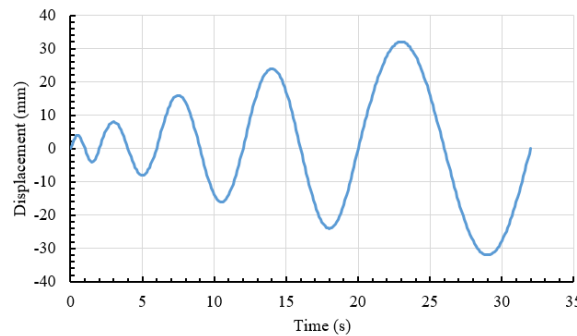


Fig. 9. Cyclic loading pattern

### 3. Result and Discussion

#### 3.1. Structural behavior

Based on eigenvalue analysis, PSSV structure braced had higher stiffness compared with unbraced PSSV seen from smaller natural period. Natural period of braced PSSV obtained from the eigenvalue analysis was 0.2778 s and 0.2155 s for first and second mode, respectively. While, unbraced PSSV had 0.5073 s and 0.4900 s natural period in first and second mode, respectively. So that, the addition of steel bracing and SPD on PSSV structure can improve the stiffness of the PSSV structure to 1.83 times bigger. Furthermore, the second stiffness of both braced and unbraced PSSV obtained by calculating the second slope of the hysteresis loop graphed in Fig.10 was utilized to investigate the other natural period of the structure. The result were 0.557 s and 0.782 s for braced and unbraced PSSV structure, respectively. The shaded part showed in Fig.8 shows the natural period range of the structures. The proposed PSSV structure was on area with relatively higher ground acceleration compared with the unbraced PSSV.

The hysteresis loop obtained from the cyclic loading analysis graphed at Fig.10 shows that braced PSSV with SPD addition has much plumper curve. The pinching curve shown at unbraced PSSV hysteresis loops indicates lower ductility and smaller energy dissipation of the structure. Furthermore, Fig.10 points out that braced PSSV also has higher equal damping ratio compared to unbraced PSSV structure. Maximum equal damping ratio calculated with Jacobsen's approach were 21.360% and 5.952% for braced and unbraced PSSV structure, respectively.

Limit state of each material used in PSSV structure was identified using static pushover analysis. The limit state was the deformation occurred at structure monitored at control node when the limit state of each materials had exceeded. The concrete crushing and PC bar yielding limit were 51.89 mm and 58.49 mm - respectively- for unbraced PSSV structure and 31.23 mm and 35.21 mm -respectively- for braced PSSV





structure. Moreover, the SPD yielding limit state for braced PSSV structure was 4.29 mm. The skeleton curve of the structures obtained from pushover analysis can be seen in Fig.11.

3.2. Seismic performance of the structure

The force and deformation relation of the maximum response under seismic excitation of PSSV structure including the limit state of each material are shown in Fig. 12. The response of unbraced PSSV structure caused the crushing at PHC pile concrete and yielding of the PC bar under all of the artificial seismic excitation. While, under recorded seismic excitation Earthquake 1 and Earthquake 2, the unbraced PSSV structure response was still below all the limit states. Interesting result can be seen at the force and displacement seismic response of braced PSSV structure with SPD addition under all of artificial and recorded seismic ground motion. The structure response due to those seismic motions did not cause any failure at the PHC pile concrete or PC bar. Otherwise, we can see that the SPD had been yielding under all seismic motions expect Earth Quake 1, the smallest earthquake used in this study. Under recorded motion Earthquake 1 and Earthquake 2, both braced and unbraced PSSV structure had lower response compared to all of the artificial motions. That was because the recorded earthquake ground motions give the low acceleration corresponding with the period enter the natural period range of both structure as showed at Fig. 8.

Based on the skeleton curves of both braced and unbraced PSSV structure with its limit states and maximum response due of the structures due to seismic excitation, as shown in Fig. 11, the application of SPD and steel bracing in PSSV structure increase the structural response. Furthermore, the braced PSSV structure had lower drift ratio due to the seismic excitations compared with unbraced one. It can be seen from the maximum displacement occurred under the seismic motions. Maximum displacement resulted from the braced PSSV structure was below 20 mm under all seismic motion, while unbraced PSSV structure exceeded the displacement of 100 mm under the seismic excitation. It indicate that the additional steel bracing can increase the structural stiffness that reduces the structural drift and the application SPD will further reduce the structural drift.

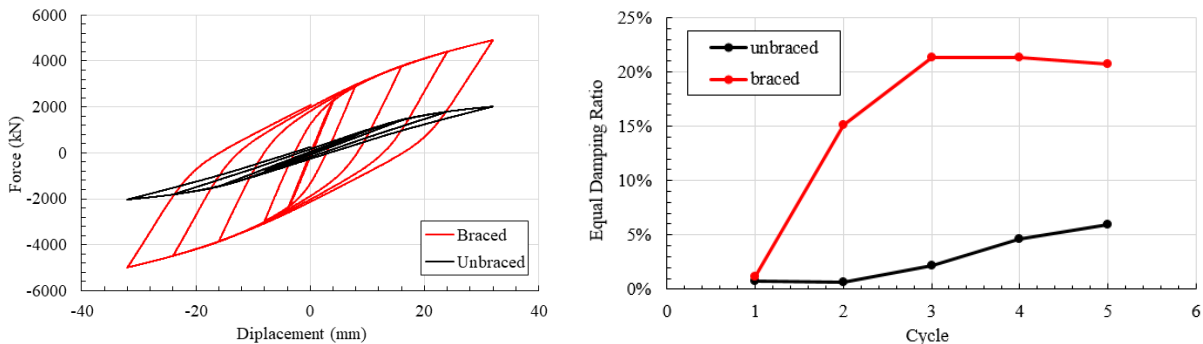


Fig. 10 – The hysteresis loop (left) and equal damping ratio (right)

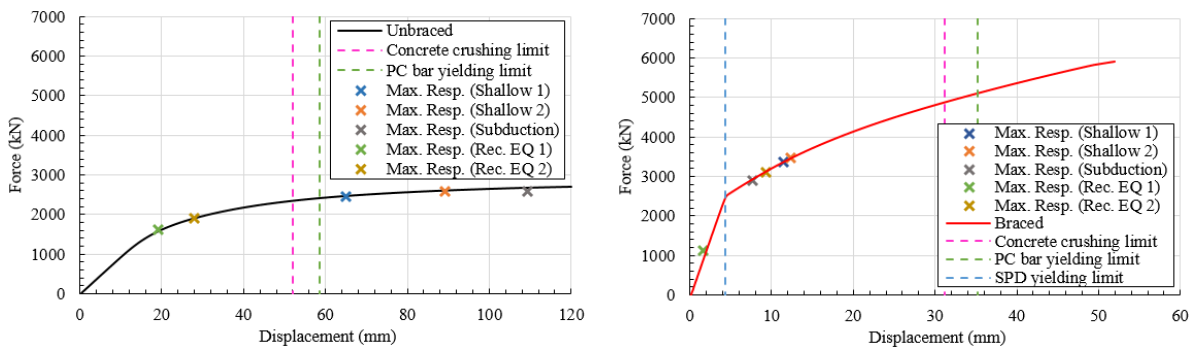
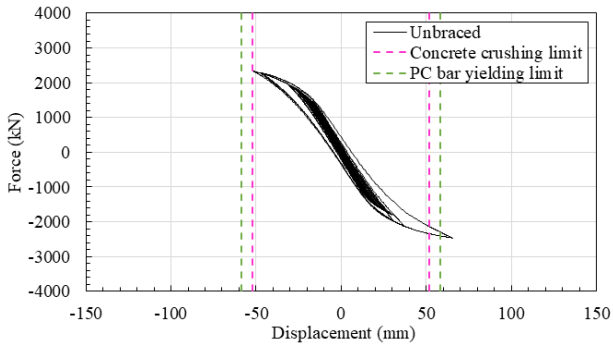
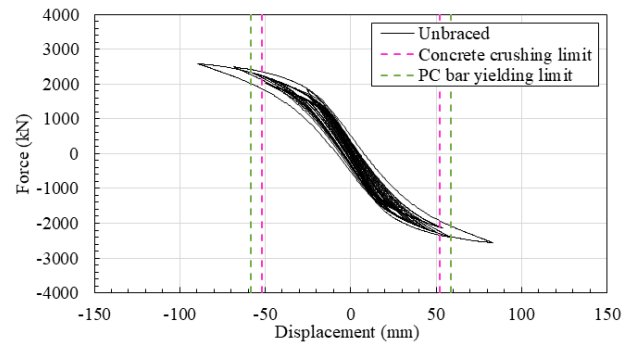
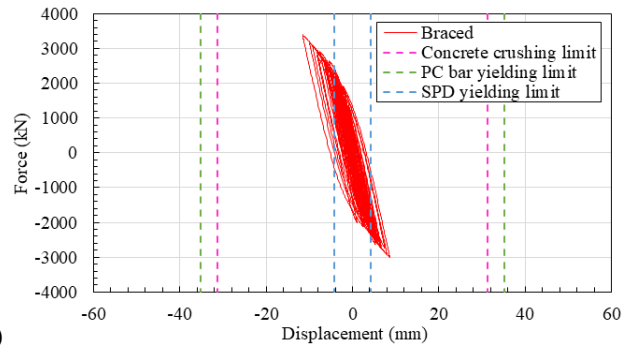


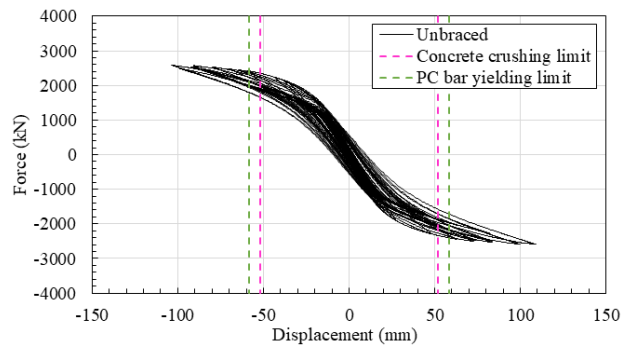
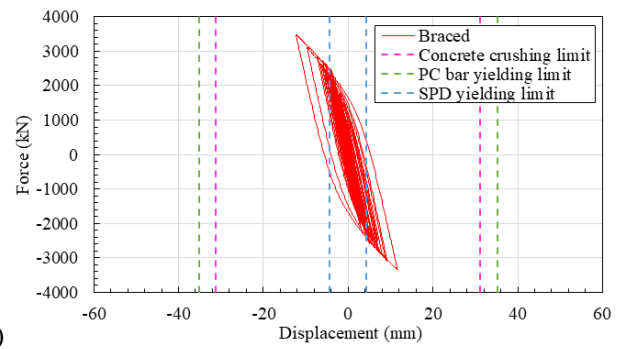
Fig. 11 – The skeleton curve and the limit state under static pushover analysis



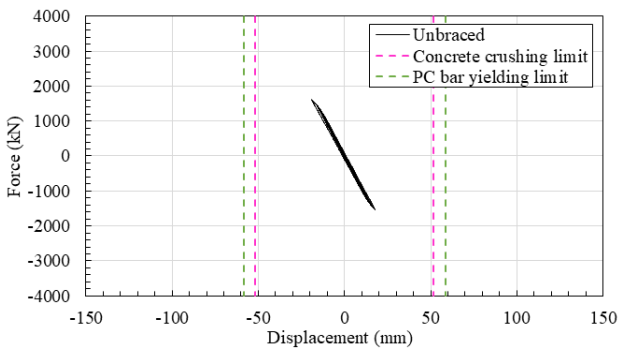
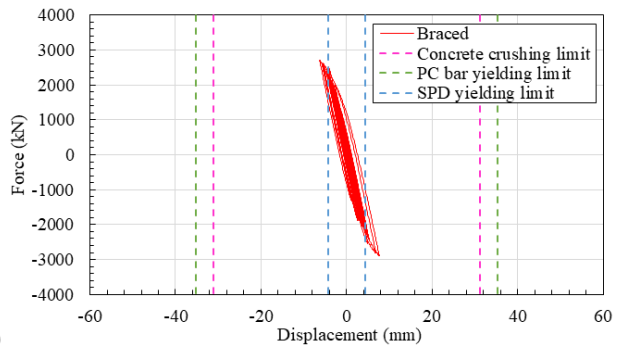
(a)



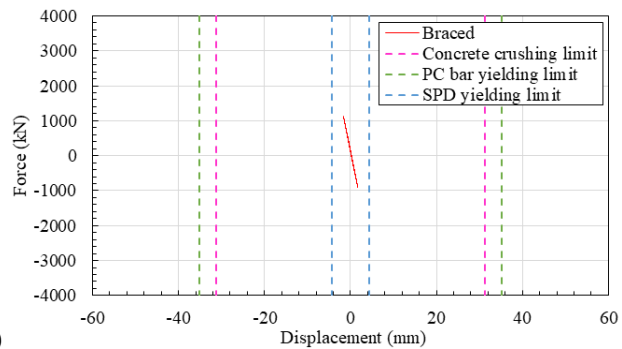
(b)



(c)



(d)



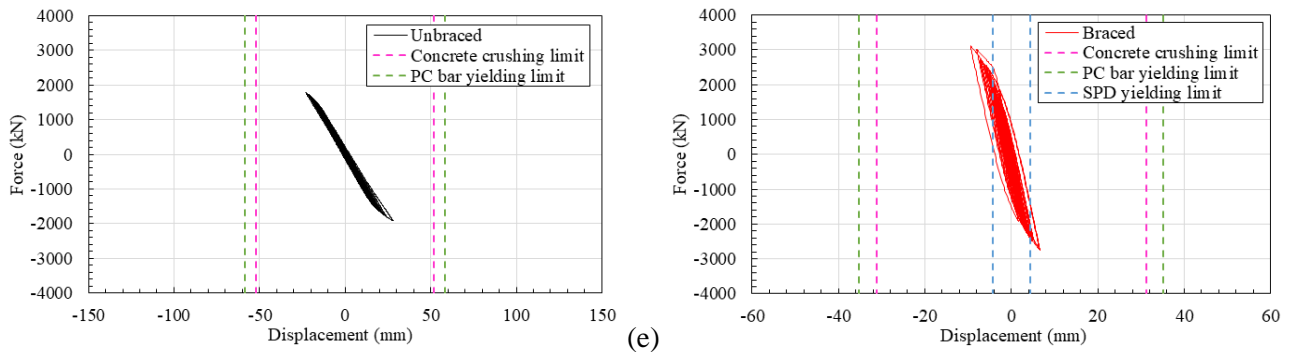


Fig. 12 – The force and displacement seismic response under seismic ground motion: (a) Shallow 1, (b) Shallow 2, (c) Subduction, (d) Earthquake 1, (e) Earthquake 2

## 4. Conclusion and Recommendation

### 4.1. Conclusion

PSSV structure braced with SPD addition performed well successfully. This proposed structure could produce much higher energy dissipation compared to the unbraced PSSV. Based on the numerical analysis results including eigenvalue, pushover, cyclic loading and dynamic time history analysis using five synthetic ground motions, the proposed structure had the following behaviors and performances:

- Braced PSSV structure with SPD addition had higher stiffness compared with unbraced PSSV structure. Natural period range of braced and unbraced PSSV structure were 0.215 s – 0.557 s and 0.490 s – 0.782 s. The application of bracing and SPD at the PSSV structure resulted 1.83 times higher stiffness than without bracing and SPD.
- The proposed PSSV structure had much higher energy dissipation than unbraced PSSV structure. It was indicated by the higher equivalent damping ratio and the plumper curve of hysteresis loop of the braced PSSV compared to the unbraced PSSV. The braced and unbraced PSSV structure can achieve the equivalent damping ratio around 21% and 6%, respectively.
- SPD addition on the PSSV structure connected by the steel bracing increase the strength of the structure. No concrete crushing and PC bar yielding occurred at braced PSSV structure due to all of seismic ground motion prepared for this study except Earthquake 1. While, crushing of PHC pile concrete and yielding of PC bar strand occurred at unbraced PSSV structure due to all of the artificial motions. No unbraced PSSV limit states was exceeded under the recorded motions.
- The recorded earthquake ground motions give the low acceleration corresponding with the period entering the natural period range of both structure so that both recorded motion of Earthquake 1 and Earthquake 2 gave the lower response compared to all of the artificial motion.
- Additional steel bracing and SPD can reduces the structural drift significantly. That was indicated from the maximum displacement occurred due to the seismic excitation i.e. below 20 mm under over 100 mm for braced and unbraced PSSV, respectively.
- The result of this study shows that the proposed PSSV structure braced with SPD addition had significantly higher seismic performance than the ordinary unbraced PSSV structure commonly used in elevated highway or railway infrastructure in Indonesia. So, the combination of SPD and steel bracing successfully increase the strength and the stiffness of the PSSV structure so that the structure can be more feasible in serving the traffic load and have lower vulnerability to the earthquake.



#### 4.2. Recommendation

Some further research related this study can improve the development and investigation of high seismic performance PSSV:

- (a) The effect of soil structural interaction and the shear failure effect of PHC Pile need to be considered for the next research
- (b) Study of energy dissipation optimization of PSSV structure by varying the SPD strength need to be conducted

### 5. Acknowledgement

The author gratefully acknowledge to Departement of Civil and Engineering, Universitas Gadjah Mada and PT. Wijaya Karya Beton that had support and funded this research.

### 6. References

- [1] M. Asrurifak, "Peta Gempa Indonesia 2017 dan Aplikasinya Untuk Perencanaan Gedung dan Infrastruktur Gempa," *Work. Pengurangan Risiko Bencana Gempa Kota Surabaya Jawa Timut ITS Surabaya*, pp. 1–73, 2017.
- [2] Reuters, "Quake damage to Indonesia's Lombok exceeds \$342 million as deaths top 400," 2018. [Online]. Available: <https://www.reuters.com/article/us-indonesia-quake/quake-damage-to-indonesias-lombok-exceeds-342-million-as-deaths-top-400-idUSKBN1KY0UM>.
- [3] Reuters, "Catastrophe in Sulawesi," 2018.
- [4] Wikipedia, "Gempa bumi Halmahera 2019," 2019. [Online]. Available: [https://id.wikipedia.org/wiki/Gempa\\_bumi\\_Halmahera\\_2019](https://id.wikipedia.org/wiki/Gempa_bumi_Halmahera_2019).
- [5] G. Benzoni, A. M. Budek, and M. J. N. Priestley, "EXPERIMENTAL INVESTIGATION OF DUCTILITY OF IN-GROUND HINGES IN SOLID AND HOLLOW PRESTRESSED PILES," no. November, 1997.
- [6] W. Taksinrote, "Seismic Performance of Pretensioned Spun High Strength Concrete Piles," THE UNIVERSITY OF BRITISH COLUMBIA, 2001.
- [7] A. Kurniadi, I. F. Rosyidin, H. Indarto, and I. D. Atmono, "Desain struktur slab on pile," *J. Karya Tek. Sipil*, vol. 4, no. 4, pp. 57–68, 2015.
- [8] A. M. Budek and M. J. N. Priestley, "Experimental analysis of flexural hinging in hollow marine prestressed pile shafts," vol. 47, no. 1, pp. 1–20, 2005.
- [9] S. Mazzoni, F. McKenna, M. H. Scott, and G. L. Fenves, "OpenSees command language manual," *Pacific Earthq. Eng. Res. Cent.*, p. 451, 2006.
- [10] C. Irawan, R. I. G. Putu, and P. Suprobo, "THE EXPERIMENTAL INVESTIGATION OF FAILURE MECHANISM OF SPUN THE EXPERIMENTAL INVESTIGATION OF FAILURE MECHANISM OF SPUN PILE DUE TO MONOTONIC LOADING USING NEHRP 2000," no. December, 2016.
- [11] Y. Ohta, H. Kaneko, M. Kibayashi, and M. Yamamoto, "Study On Shear Panel Dampers Using Low Yield Strength Steel Applied To Reinforced Concrete Buildings Assemblies With A Shear Panel Damper Subjected To Horizontal," 2004, no. 2228.
- [12] B. Sunardi, "Percepatan Tanah Sintetis Kota Yogyakarta Berdasarkan Deagregasi Bahaya Gempa," *J. Lingkungan. dan Bencana Geol.*, vol. Vol. 6 No., pp. 211–228, 2015.
- [13] D. M. Boore, "Simulation of Ground Motion Using the Stochastic Method," *Pure Appl. Geophys.*, vol. 160, pp. 635–676, 2003.
- [14] H. B. Seed and I. M. Idriss, "Soil modulus and damping factors for dynamic response analyses," p. Report No. EERC 70-10, 1970.
- [15] L. Jacobsen S., "Steady forced vibrations as influenced by damping," *Trans. 1930;52(15)169(181)*.